Optics and Lasers in Engineering 49 (2011) 366–370

Contents lists available at ScienceDirect

Optics and Lasers in Engineering

journal homepage: www.elsevier.com/locate/optlaseng

Experimental study on the micromechanical behavior of a PBX simulant using SEM and digital image correlation method

Zhongbin Zhou, Pengwan Chen *, Fenglei Huang, Siqi Liu

State Key Laboratory of Explosion Science and Technology, Beijing Institute of Technology, Beijing 100081, China

ARTICLE INFO

Article history:
Received 1 January 2010
Received in revised form
1 November 2010
Accepted 3 November 2010
Available online 26 November 2010

Keywords:
Heterogeneous deformation field
Digital image correlation
Polymer bonded explosive simulant
Micromechanical behavior

ABSTRACT

The micro-scale mechanical behavior of a polymer-bonded explosive (PBX) simulant was experimentally studied using a scanning electron microscope (SEM) imaging system and digital image correlation (DIC) method. The semi-circular bend (SCB) test was chosen for the study. During the testing, a series of SEM images of the specimen was acquired in situ. The natural micro-structural features of the specimen were used as random speckle pattern for DIC analysis. The displacement and strain fields at the area of interest were obtained by DIC. The deformation and damage of PBX were analyzed. Heterogeneous strain fields demonstrated the damage evolution underneath the specimen surface and predicted possible micro-crack growth. Based on the contour plots of the correlation coefficient, the formation and extension of microscopic cracks were quantitatively analyzed.

1. Introduction

Polymer-bonded explosive (PBX) is a composite material containing a large volume of crystalline high explosive (90–95% by weight) mixed with a small percentage of soft binder. It is used in a wide variety of applications, ranging from rocket propellants to the main explosive charge in munitions. PBX is carefully designed to give optimum explosive power and sufficient mechanical strength, as well as a range of safety features. Recently, the mechanical properties and failure mechanisms of PBX have been studied [1–4]. These studies were qualitative analyses of PBX properties, with very little relation to the deformation field of the loaded materials. The fracture behavior and mechanical properties of PBX are known to be highly dependent on its microstructure; therefore, its performance at the micro-scale level should be experimentally characterized at the equivalent size scale. One challenge of such small-scale testing is the measurement of strains at a micro-size area. A conventional strain measurement method such as a strain gauge is not applicable at this scale. Moiré techniques are possible [5], but the fabrication of a fine specimen grating is difficult and expensive. Therefore, the development of a convenient experimental method for deformation measurement at micro-scale is necessary.

The digital image correlation (DIC) method is widely used in experimental mechanics as an effective tool for full field measurement. This method is easy to manipulate and can provide satisfactory resolution of displacement and strain fields at a macro-scale [6–9]. At this scale, spraying white and black paints alternatively normally generates a random grey scale pattern for DIC analysis. To use the DIC for microscopic deformation measurement, digital images must be obtained from high-magnification imaging systems, such as an optical microscope, scanning electron microscope (SEM), or an atomic force microscope (AFM). In the literature, Rae et al. [10–12] first studied the microscopic deformation and fracture behavior of PBX by DIC combined with an optical microscope. However, the magnifying power of optical microscope is limited by the principle of light up to 1000 ×, usually with the area of view in the sub-millimeter range. An AFM can provide images with high resolution; however, incorporating a loading stage in an AFM chamber is difficult because of the spatial limitation. A SEM can provide a wide range of magnification, from 30 × to 100,000 ×, and the SEM chamber is large to work with. In Refs. [13,14] SEM images were digitally processed by DIC, and the deformation behavior of PBX under uniaxial loading was studied. Knowledge of the localized strain field in heterogeneous material is very useful for the investigation of the microscopic fractures and failure mechanisms that govern the macroscopic mechanical behavior of materials. Therefore, further research is needed to investigate the processes of damage evolution and failure of PBX.

In this work, a semi-circular bend test was chosen for the study. In order to study the micromechanical behavior of PBX, the DIC method was combined with a SEM imaging system incorporated with a loading stage to study the deformation field of the sample at a micro-scale. This method was employed in two applications: (1) to characterize the micromechanical behavior of PBX and (2) to study the strain concentration around the crack tip of a semi-circular specimen.

* Corresponding author.
E-mail address: pwchen@bit.edu.cn (P. Chen).

0143-8166/$ - see front matter Crown Copyright © 2010 Published by Elsevier Ltd. All rights reserved.
doi:10.1016/j.optlaseng.2010.11.001

2. Experiments

2.1. Specimen preparation

Owing to safety requirements, a simulation material of PBX was used in the study. The samples were produced in a steel-press mold. In order to obtain disc-shaped samples, 200 MPa pressure was applied for an hour in the steel-press mold at a temperature of 100 °C.

To reveal the microstructure of the sample, polishing was required. First, samples were ground using fine emery papers (#600) to obtain a flat surface. Next, polishing was carried out on the polishing machine using a fine polishing paste. Finally, gold was sprayed onto the sample surface to form a conductive layer.

The samples were made from a relatively weak, brittle material, and the test specimens were machined from the original disc sample. Thus, damage induced during this period could be significant. Great care was therefore taken to avoid additional damage.

2.2. Semi-circular bend (SCB) test

A tensile load may cause rupture from an existing defect away from the crack tip. However, machining a specimen required for tensile loading is difficult because of its low strength. Consequently, test should be conducted with compressive loading when tensile fractures are induced. In order to satisfy this requirement, the SCB test was proposed [15]. The SCB sample with a single edge notch was subjected to a three-point bending load (as shown in Fig. 1). The sample geometry is advantageous for convenient sample preparation and for relative ease of experimentation. In this paper, we focus on the field deformation in the tip region of the pre-notch. The local region (labeled "Area 0") was observed by SEM in each loading step, and the recorded images were digitally processed by DIC to extract the strain field. These examinations were conducted with the aim of revealing the strain localization responding to specimen damage, even without any obvious signs of cracks, and predicting the propagation of the induced crack, along with the possible developing path, in a splitting fracture of brittle failure.

2.3. SEM system

The SEM system used in this work was a model S-570 from Hitachi Corporation. A loading stage was installed inside the SEM chamber, which enabled the SEM to acquire images during each loading step. This system is capable of applying tensile or compressive load of up to 2000 N, either by motor-driven or manual-driven gears. In the SEM system, the accelerator voltage of 25 KV and the probe current of 100 μA were chosen to obtain the images. Image size used was 840×960 pixels^2. The advantage of the loading stage design is that the whole assembly of the loading stage and the specimen can be translated inside the SEM chamber, which enables the specimen to be moved back to the original position after each incremental loading step. During the testing, the specimen was loaded step by step. After each increment, the loading was paused to acquire the SEM image. The imaging area of the specimen was carefully adjusted so that the images were always taken from the same area on the sample surface after each step of loading. The position adjustment was based on the tracking of one particle, chosen as the reference marker, in order to eliminate spatial distortions during each loading step. Therefore, a series of SEM images of the specimen was acquired in situ over the same area of interest.

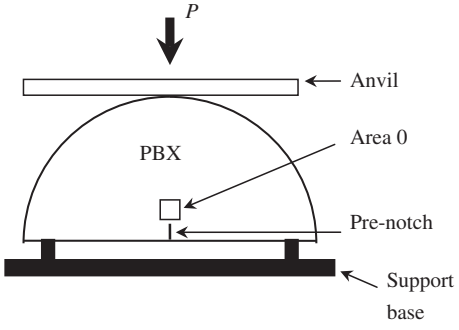

Fig. 1. Semi-circular bend test geometry.

2.4. Principle of the digital image correlation

DIC operates through the mathematical comparison of two sub-images from a larger pair of displaced images. The deformation field can be obtained by comparing a resource subset from a reference digital image with a target subset from a deformed image [16,17]. The primary assumption of DIC is that the essential characteristics of the speckle pattern remain the same before and after deformation to determine the distortion of a small region. This method uses the correlation coefficient C as a description parameter [18]:

$$C = 1 - \frac{\sum[f(x,y)-\bar{f}][g(x',y')-\bar{g}]}{\sqrt{\sum[f(x,y)-\bar{f}]^2}\sqrt{\sum[g(x',y')-\bar{g}]^2}} \quad (1)$$

where (x, y) and (x', y') are Cartesian coordinates of the resource and target points located in the reference and deformed images, respectively; $f(x, y)$ and $g(x', y')$ are the grey values of the subset in the non-deformed and deformed images, respectively; and $\bar{f}$ and $\bar{g}$ are the ensemble averages. The magnitude of correlation coefficient C varies from 0 to 1, with 0 signifying a perfect match between the two images. When damages or cracks develop in the small region during deformation, the local characteristic of the speckle images is changed, and the correlation coefficient becomes bigger than other areas where no damage and crack are present. In our work, the value of C is smaller than 0.01 in the area of interest (as shown in Fig. 6), indicating that the two speckle images captured before and after a deformation match each other well. Therefore, the speckle pattern converted from the SEM image was suitable for DIC analysis.

3. Results and discussion

3.1. DIC analysis of deformation

For the SCB test, a specimen 20 mm in diameter and 10 mm in thickness was machined from a disc sample. A pre-notched edge 0.9 mm in length and 0.2 mm in width was fabricated using a blade. For each loading step with a force increment approximately $P=50$ N, the near region (as shown in Fig. 2) around the tip of the preset crack was magnified by SEM to observe the surface topography in situ and to record the images during the compressive load. The interest region "Area I" was analyzed by DIC to match with the initial image recorded before deformation. The subset size of 29×29 pixels^2 and step size of 4 pixels were chosen for the DIC analysis. The tensile strain fields for selected steps at different loading levels are shown in Fig. 3. As evident in the figure, the strain field is not uniform. The maximum strain is concentrated around the tip of pre-crack. Moreover, the localized strain band is evidently propagating and evolving along the preset notch direction with increase of the external force. The fracture route is believed to follow the orientation of prefabricated crack.

At load $P=400$ N (Fig. 3c), the local area E shows a significant strain concentration that may be caused by the initial damage near the tip of the generated crack. With the increase of external loading, the initial crack starts from the tip of pre-crack and grows along the loading direction. In addition, real-time microscopic examination indicates that the failure began at several independent sites. The micrograph of the sample at load $P=400$ N is shown in Fig. 7. Two separate micro-cracks (Cracks 1 and 2, as indicated by arrows) are present along the loading axis. Significantly, at this loading state, Crack 2 is not around the new Crack 1 tip. Instead, it appears at a finite distance (approximately 50 μm) in front of the tip of Crack 1, showing that a decohesive zone has developed ahead of the Crack 1.

In order to further study the microscopic fracture behavior, the local region labeled "abcd" (marked in Fig. 2) was carefully examined. Fig. 4 shows the micrograph of the "abcd" region at four loading steps. At the load $P=250$ N, the particle marked A has cracked, which is likely due to impeding the propagation route of the crack M. At the same time, a failure crack N passes between the two particles marked P and Q, which may be caused by initial damage being activated, and which tends to evolve. With the increase of external compression loading, the crack M does not propagate. Nevertheless, the interfacial crack N extends uninterruptedly, as shown in Fig. 4b and c. Finally, a more typical example of filler particle fracture is shown in Fig. 4d. In this micrograph, the typical failure path (indicated by arrows) has been formed. Microscopic crack propagation is mainly along the interface of particles and matrix in this sample, especially the particle marked R.

Fig. 5 shows the tensile strain field of the "abcd" region at a micro-scale, which corresponds to the loading states wherein external forces equaled 250, 310, 400, and 450 N, respectively. The results show how the strain concentration was developed during the SCB fracture test. Moreover, the strain fields predict a transition of the damage accumulation from particle/matrix debonding to crack formation.

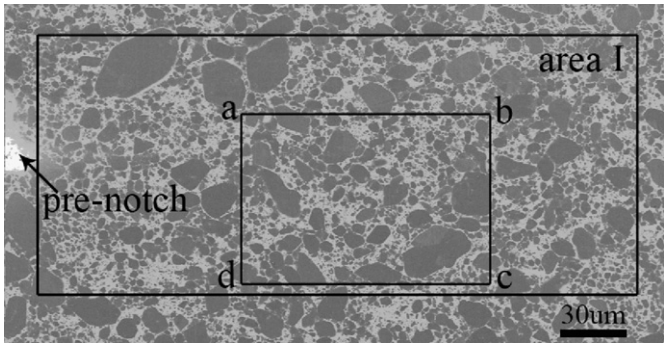

Fig. 2. SEM image of the sample obtained around the tip of pre-crack.

3.2. Fracture propagation analysis by correlation coefficient

Cracking is the most dominant mechanical failure mechanism in high explosives and affects the mechanical performance and detonation of weapon systems. However, direct observation and quantitative measurement of the deformation field associated with the formation and extension of micro-cracks are great challenges because cracks are hardly observable directly until they have grown sufficiently large. Recently, based on the application of DIC technique, the characteristics of this method have been better understood, and the initiation and propagation of cracks in explosives can be quantitatively described [19]. As discussed in Section 2.4, the correlation coefficient C is a function of the grey values of the two digital images before and after deformation. When the distortion of the small region is such that two small images match each other, the correlation coefficient is at a minimum. However, when damage or cracks develop in the small region during deformation, the correlation coefficient may not be able to attain a minimum; the value of the coefficient C becomes much bigger than in other regions where no damage or cracks are present. Generally, in DIC analysis, the correlation coefficient is only used for judging the numerical convergence in order to attain an ideal precision. In this work, the correlation coefficient was used

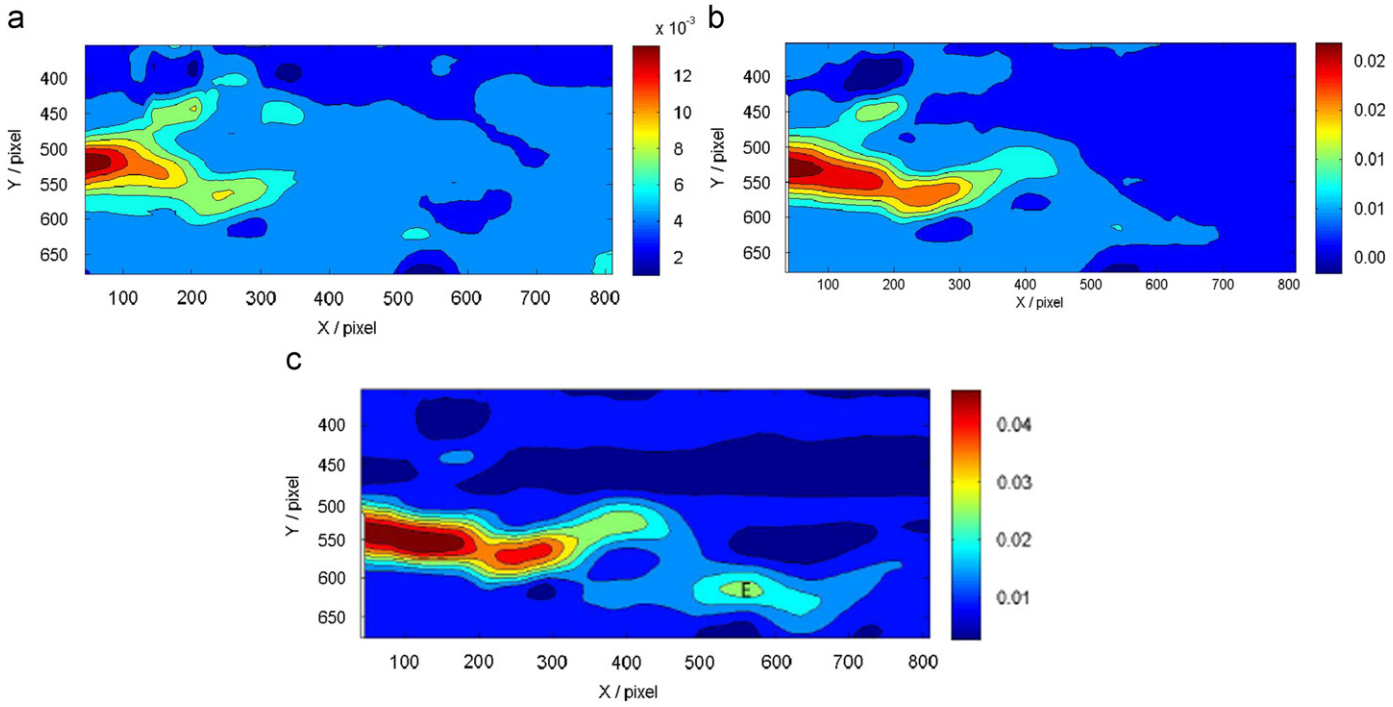

Fig. 3. Tensile strain (ε_y) contours of Area I at different loads: (a) $P=150$ N, (b) $P=250$ N, and (c) $P=400$ N.

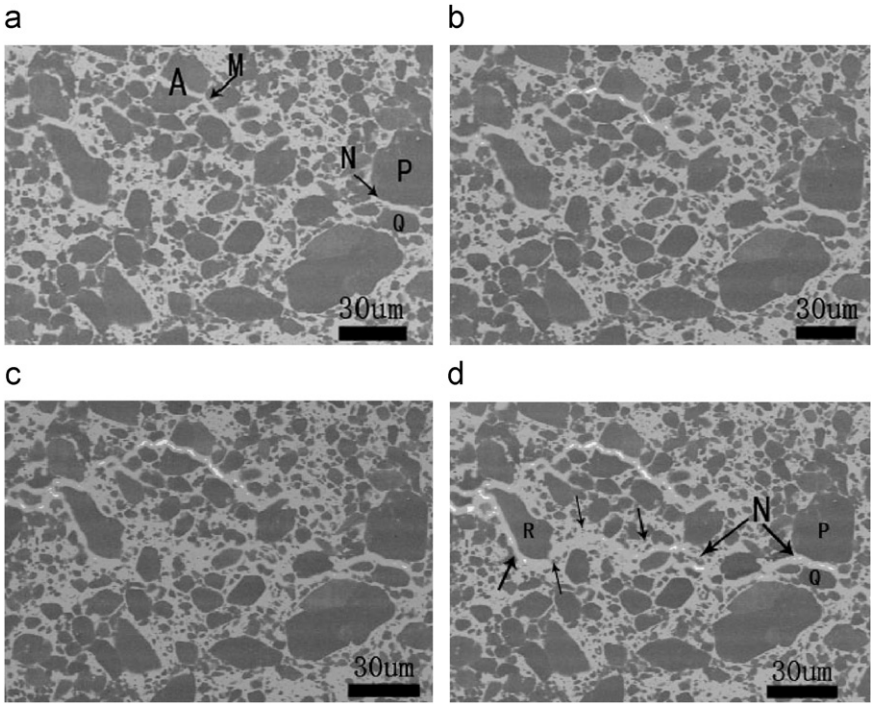

Fig. 4. Micrograph of the "abcd" region at different loads: (a) P=250 N, (b) P=310 N, (c) P=400 N, and (d) P=450 N.

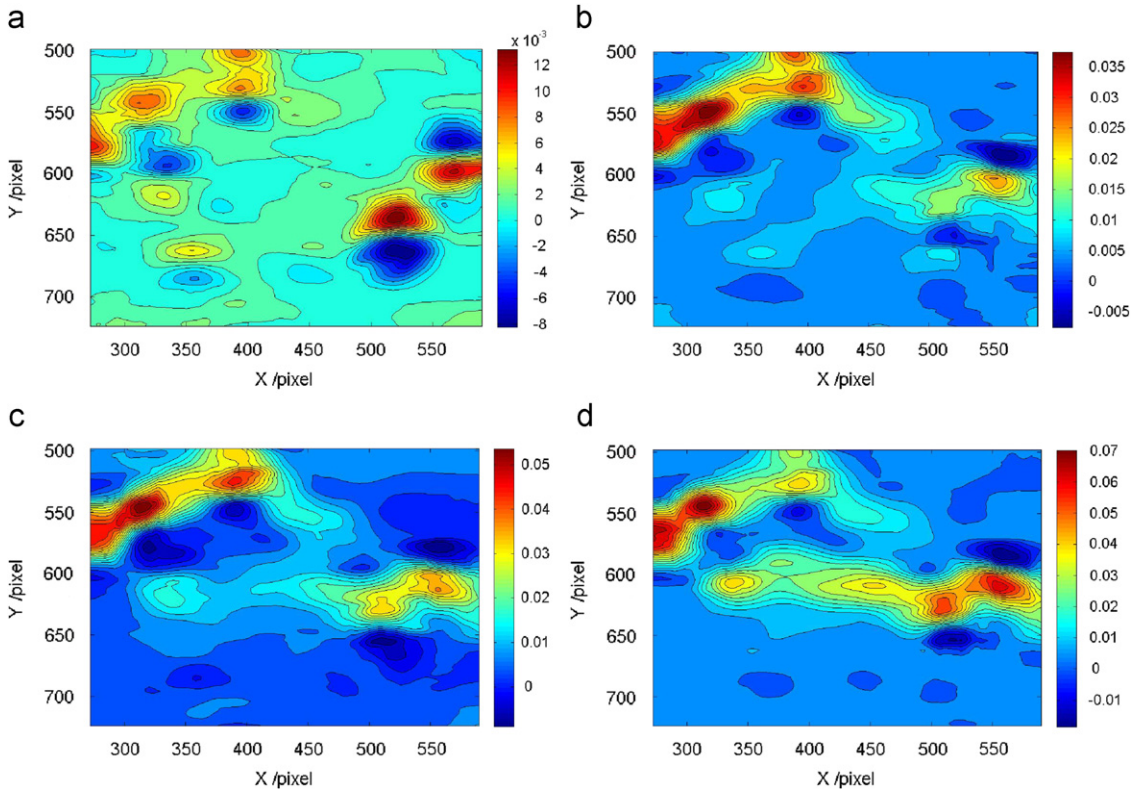

Fig. 5. Tensile strain distribution (ε_y) in the "abcd" region at different loads: (a) P=250 N, (b) P=310 N, (c) P=400 N, and (d) P=450 N.

to quantify the location and extent of cracks in the semi-circular specimen.

Fig. 6 shows the contour plot of the correlation coefficient of the sample corresponding to two selected moments. The strain fields in moments a and b are indicated in Fig. 3b and c. When damage or cracks developed in Area I during deformation, the local characteristic of the speckle images is changed, and the value of correlation coefficient becomes bigger than that in other regions where no cracks are present. In moment a, the magnitude of C is the largest in the region in front of the tip of pre-crack, indicating that microscopic crack was formed in this moment. In the subsequent moment, moment b, the cracked region grows larger. Specifically, in this

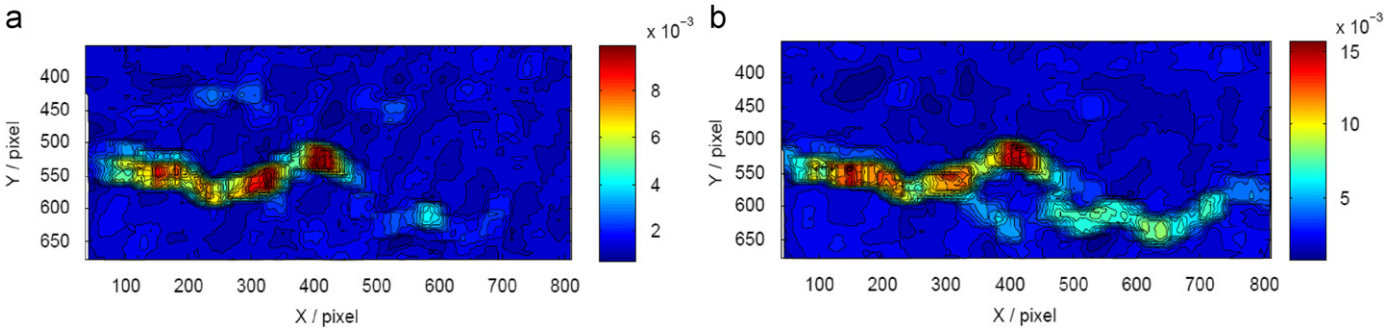

Fig. 6. Contour plot of correlation coefficient C of a semi-circular sample at two loading states: (a) P=250 N and (b) P=400 N.

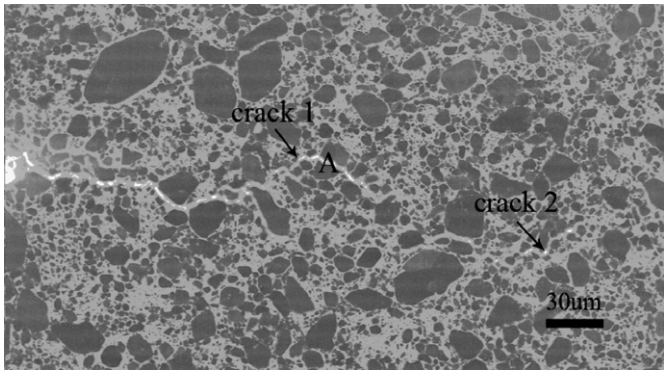

Fig. 7. Microstructure of PBX sample at load 400 N.

moment, there are two disconnected cracks present, as demonstrated in Fig. 7.

With the increase in external loading, these disconnected cracked regions enlarge and coalesce, and a single dominant crack appears along the orientation of prefabricated crack. The experimental result demonstrates that the micro-scale crack propagation in this highly particle-filled composite is mainly along the filler particle/matrix interface, as shown in Fig. 7. Interfacial debonding of particle/matrix governs the fracture of the sample. Transgranular fracture is significant in the single particle (labeled "A"); however, this phenomenon rarely occurs.

4. Conclusions

An experimental method combining SEM imaging system with DIC technique has been developed to study the full-field deformation of a PBX simulant at a micro-scale. In situ SEM images of the surface microstructures of PBX in SCB test were acquired during each incremental loading step. The microscopic deformation and fracture behavior of PBX were analyzed. In addition, the DIC technique was applied to these SEM images captured in SCB test, and the strain fields at the area of interest were obtained. In the tip region of the preset crack, the strain fields are effective in predicting the possible micro-crack growth path. The experimental results demonstrate that combining SEM with the DIC is capable of studying the deformation field of PBX at a micro-scale. The results show that cracks initiate and propagate along the particle surfaces, and the dominant fracture mode is inter-granular cracking.

Acknowledgements

This work is supported by the National Natural Science Foundation of China (under Grant no. 10832003), the NSAF (under Grant no. 11076032), the National Basic Research Program of China (under Grant no. 613830202), and the Program for New Century Excellent Talents (under Grant no. NCET-06-0159). The authors thank Professor Nie Fude of the Institute of Chemical Materials, the Chinese Physical Academy, for providing PBX mock materials. The authors also thank Dr. Ma Shaopeng of the Department of Mechanics, School of Aerospace, Beijing Institute of Technology, for providing the DIC software.

References

[1] Palmer SJP, Field JE, Huntley JM. Deformation, strengths and strains of failure of Polymer bonded explosives. Proc R Soc Load A 1993;440:399–419.
[2] Chen PW, Huang FL, Ding YS. Microstructure, deformation and failure of polymer bonded explosives. J Mater Sci. 2007;42:5272–80.
[3] Chen PW, Xie HM, Huang FL, et al. Deformation and failure of polymer bonded explosives under diametric compression test. Polym Test 2006;25:333–41.
[4] Chen PW, Huang FL, Zhang Y. Brazilian test and its application in the study of the mechanical properties of explosives. Acta Armament 2001;22(4): 533–7. (in Chinese).
[5] Xie HM, Shi H, Chen PW, et al. An experimental study on creep deformation of PBX with laser moiré interferometry method. Fract Strength Solids 2006;6: 1037–42.
[6] Peters WH, Ranson WF. Digital imaging techniques in experimental stress analysis. Opt Eng 1982;21(3):427–31.
[7] Pan B, Qian KM, Xie HM, et al. Two-dimensional digital image correlation for in-plane displacement and strain measurement: a review. Meas Sci Technol 2009;20:062001.
[8] Chu TC, Ranson WF, Sutton MA, et al. Application of digital image correlation techniques to experimental mechanics. Exp Mech 1985;25(3):232–45.
[9] Sutton MA, McNeill SR, Helm JD, et al. Advances in two dimensional and three dimensional computer vision. In: Rastogi PK, editor. Topic in Applied Physics, 77. Springer Verlag; 2002. p. 323–72.
[10] Rae PJ, Goldrein HT, Palmer SJP, et al. Studies of the failure mechanisms of polymer bonded explosives by high resolution moire interferometry and environment scanning electron microscopy. In: Proceedings of the 11th international detonation symposium; 1998.
[11] Rae PJ, Palmer SJP, Goldrein HT, et al. White light digital image cross-correlation analysis of the deformation of composite materials with random microstructure. Opt LaserEng 2004;41:635–48.
[12] Rae PJ, Goldrein HT, Palmer SJP, et al. The use of digital image cross-correlation to study the mechanical properties of a polymer bonded explosive (PBX). In: Proceedings of the 12th international detonation symposium; 2002.
[13] Li M, Zhang J, Xiong CY, et al. Damage and fracture prediction of plastic bonded explosive by digital image correlation processing. Opt Laser Eng 2005;43: 856–68.
[14] Liu ZW, Xie HM, Li KX, et al. Fracture behavior of PBX simulant subject to combined thermal and mechanical loads. Polym Test 2009;28:627–35.
[15] Chong KP, Kuruppu MD. New specimen for fracture toughness determination for rock and other materials. Int J Fract 1987;26:R59–62.
[16] Pan B, Xie H. Full-field strain measurement based on least-square fitting of local displacement for digital image correlation method. Acta Opt Sin 2007: 1980–86.
[17] Pan B, Xie HM, Guo ZQ. Full-field strain measurement using a two-dimensional Savitzky–Golay digital differentiator in digital image correlation. Opt Eng 2007;46(3):033601–10.
[18] Ma SP, Jin GC, Pan YS. Deformation measurement method for rock materials based on natural speckle pattern. Chin J Rock Mech Eng 2002;21(6): 792–6. in Chinese.
[19] Liu C, Darla GT, Manuel LL, et al. Macroscopic crack formation and extension in pristin and artificially aged PBX 9501. In: Proceedings of the 14th international detonation symposium; 2010.